

Julita KRASSOWSKA • Marta KOSIOR-KAZBERUK • Marta SŁOWIK •
Amanda AKRAM

SUSTAINABLE FUTURE OF CONSTRUCTION: THE POTENTIAL OF CONCRETE WITH BASALT MINI-BARS AS REINFORCEMENT

Julita **Krassowska** (ORCID: 0000-0001-9209-1285) – *Faculty of Civil and Environmental Engineering, Bialystok University of Technology, Bialystok, Poland*

Marta **Kosior-Kazberuk** (ORCID: 0000-0001-8171-2242) – *Faculty of Civil and Environmental Engineering, Bialystok University of Technology, Bialystok, Poland*

Marta **Słowik** (ORCID: 0000-0001-9627-3625) – *Faculty of Civil Engineering and Architecture, Lublin University of Technology, Lublin, Poland*

Amanda **Akram** (ORCID: 0000-0001-5619-2927) – *Faculty of Civil Engineering and Architecture, Lublin University of Technology, Lublin, Poland*

Correspondence address:

Wiejska Street 45E, 15-351 Bialystok, Poland

e-mail: j.krassowska@pb.edu.pl

ABSTRACT: The paper concerns the influence of basalt minibars on the subcritical and critical behaviour of test specimens made of concrete with low-emission cement. Low-emission cement produces lower emissions of greenhouse gases and other pollutants than traditional cement. Analyses were conducted on changes in fracture mechanics parameters depending on the content of microfibers in the concrete mix (0, 2, 4, 8 kg/m³), the type of cement used, and the water-to-cement ratio (w/c). It was demonstrated that concrete reinforced with basalt microfibers exhibits increased resistance to crack initiation and propagation. An increase in the stress intensity factor was observed for CEMI 42.5R concretes at $w/c=0.5$ by 27%, at $w/c = 0.4$ by 62%, and for CEM II 42.5R/A-V concretes at $w/c = 0.5$ by 29%, and at $w/c = 0.4$ by as much as 30%. It was shown that the addition of microfibers to concrete made with low-emission cement significantly increases the mechanical parameters of this material.

KEYWORDS: concrete, basalt minibars, post-cracking behaviour, fracture parameters

Introduction

The continuous search for sustainable and resilient construction materials has led to the exploration of innovative alternatives to traditional reinforcement solutions. One such promising solution is the incorporation of basalt minibars as a reinforcing component in concrete structures. This paper describes a comprehensive examination of the mechanical behaviour of concrete when reinforced with basalt minibars, providing suggestions on its potential use in the construction industry. Multi-component pozzolanic cement CEM II was used, which is a universal cement. The composition of CEM II cement has been developed in accordance with the principles of sustainable development, and thanks to the use of decarbonised raw materials, this has allowed to reduce the carbon footprint, expressed by carbon dioxide emissions per ton of produced cement compared to CEM I 42.5 R by 27%.

The production of cement is responsible for approximately 5% of the world's anthropogenic carbon dioxide emissions into the atmosphere (Batog et al., 2022). It is estimated that the production of one ton of clinker results in emissions of approximately 800 to 850 kg of CO₂ into the atmosphere. Limiting these emissions is becoming increasingly significant in the context of climate change. This was made possible through the modernisation of the clinker firing process, the introduction of alternative fuels replacing coal, and the widespread use of cement with non-clinker main components instead of Portland cement CEM I, mainly these were multi-component Portland cement CEM II/A, B, and cement CEM III/A. Cement CEM II 42.5R/A-V is a type of Portland cement characterised by certain drawbacks, which may include low compressive strength, increased shrinkage, sensitivity to environmental conditions, and low stability.

To prevent the drawbacks of concretes with CEM II 42.5R/A-V cement, it is possible to use dispersed reinforcement. Basalt microbars, obtained from natural basalt rock, are considered a viable alternative to conventional reinforcement materials such as steel. The unique properties of basalt, including its high tensile strength, corrosion resistance, and abundance, make it an attractive candidate for sustainable construction practices. Regarding basalt concrete reinforcement, there are two primary types of dispersed reinforcement: chopped basalt fibres (BF) and a novel product known as minibars (small bars with a diameter of 1mm) (MB).

Research on basalt fibre reinforced concrete (BFRC) has predominantly focused on its fundamental mechanical properties, indicating that the addition of fibres is generally beneficial up to approx. 0.3–0.5% by volume, but becomes detrimental thereafter (Iyer et al., 2015; Jiang et al., 2014). The optimal content varies across different concrete types – in the case of microbars (MB), it is up to 4% by volume (Patnaik et al., 2013). While the influence on compressive strength is not typically significant, the primary advantage of using both basalt fibres (BF) and (MB) in concrete compression lies in achieving a transition from a brittle to a more ductile failure mode. Basalt minibars (MB) are obtained by melting and drawing basalt rocks. Basalt ore is created from molten rock magma and formed in conditions of high temperature, high pressure, and subsequent ambient pressure reduction. It is characterised by excellent chemical and thermal stability (Kabay, 2014; Wei et al., 2010). As a result, basalt minibars inherit the properties of basalt ore, including exceptional thermal stability, resistance to corrosion, excellent heat insulation and sound absorption as well as low moisture absorption. Furthermore, basalt minibars are characterised by high values of strength and Young's modulus (Abbas Ashour Alaraza et al., 2022; Patnaik et al., 2013).

Branston et al. (2016a) studied basalt fibres, known for their eco-friendly production and strong mechanical properties in terms of their impact on concrete mechanics – by comparing bundle dispersion fibres with minibars. Three fibre quantities were used in concrete specimens and subjected to flexural and drop-weight impact tests. Observations performed with the use of electron microscopy revealed that while both fibre types enhanced pre-cracking strength, only minibars improved post-cracking behaviour, possibly due to polymer protection. Another study performed by Branston et al. (2016b) determined that chopped basalt fibres showed promising results in mitigating early-age cracking caused by plastic shrinkage in concrete. This was evidenced by reduced free shrinkage and restrained crack growth, with the latter effect being more pronounced at lower water-to-cement ratios.

Concrete's cracking resistance hinges on micro-crack zone fracture processes. Plain concrete crack formation is analysed via basic fracture parameters, which are crucial in post-tension critical work. Steel bars notably influence crack development. Słowik and Błazik-Borowa (2011) studied

their impact on stress distribution within fracture zones, highlighting their effectiveness in transferring tensile stresses based on reinforcement ratio (Słowik, 2019). Research now emphasises non-metallic reinforcement, like dispersed reinforcement.

Interest in alternative reinforcement materials for concrete structures has grown, yet a notable gap exists in understanding the post-cracking behaviour specific to basalt minibars reinforced concrete. While various studies have explored basalt's potential, few focus on systematically investigating concrete structures reinforced with basalt minibars post-cracking. Existing literature mainly addresses basalt fibres or traditional-sized rebars, overlooking minibars' unique characteristics and benefits. Basalt minibars, with smaller diameters, pose distinct challenges and opportunities in crack propagation and load distribution. The gap lies in understanding how minibars influence concrete's post-cracking behaviour. To address this, investigations were conducted using two types of cement: CEM I and CEM II. The study aimed to assess how different basalt minibar contents (2, 4, and 8 kg/m³) affect concrete's toughness and post-cracking behaviour. Three-point bending tests were performed, hypothesising that basalt minibars impact fracture and mechanical properties. This research could offer insights into popularising low-emission cement and mitigating drawbacks through cost-effective basalt minibar reinforcement, there by promoting material functionality while reducing environmental pollution.

Experimental Investigation

Experimental Program

The main aim of the research was to analyse the influence of basalt minibars on the mechanical properties and fracture parameters of concrete. The research was conducted in 16 series, as presented in Table 1. The variable parameters were water-to-cement ratio and minibars content. The series was divided into four groups, with four series in every group characterised by different minibars contents, i.e. 0, 2, 4, and 8 kg/m³:

- first group with cement type CEM I 42.5 and $w/c = 0.5$,
- second group with cement type CEM I 42.5 and $w/c = 0.4$,
- third group with cement type CEM II 42.5R/A-V and $w/c = 0.5$,
- fourth group with cement type CEM II 42.5R/ A-V and $w/c = 0.4$.

Table 1. Research program

Series	Type of cement	w/c	Minibars content V_f [kg/m ³]
M1	CEM I 42.5	0.5	0
M2			2
M3			4
M4			8
M5		0.4	0
M6			2
M7			4
M8			8

Series	Type of cement	w/c	Minibars content V_f [kg/m ³]
M9	CEM II 42.5R/ A-V	0.5	0
M10			2
M11			4
M12			8
M13		0.4	0
M14			2
M15			4
M16			8

Materials

The geometry and the properties of basalt minibars are presented in Table 2, and the view of minibars is presented in Figure 1.

Table 2. Properties of minibars

Property	Basalt minibars
Fiber shape	straight
Length (mm)	50
Diameter (mm)	0.7
Tensile strength (MPa)	>1000
Elastic modulus (GPa)	42
Density (kg/m ³)	2650



Figure 1. Basalt minibars

The cement (CEM I 42.5R or CEM II 42.5R/A-V) content was the same in all tested concretes, i.e. 320 kg/m³. The aggregate mix contained 38% of the 0-2 mm fraction and 62% of the 2-16 mm fraction. The minibars were added as a replacement for part of the coarse aggregate by volume.

Methods

Compressive strength f_c of concrete was tested on cubic samples with a size of 100 mm; concrete flexural strength $f_{ct,fl}$ was tested on 100×100×400 mm samples, Young's modulus E_{cm} was determined on cylindrical specimens with a diameter of 150 mm and a height of 300 mm.

The fracture performance of concrete specimens, i.e. those reinforced with minibars and unreinforced control concrete, was assessed following the guidelines provided by RILEM (Determination of the fracture energy of mortars and concretes by means of three-point bend tests on notched beams, 1985). Notched 100×100×400 mm beams were employed for the three-point bending test. At beam midpoint, an initial saw-cut notch was made, with a depth of 30 mm and a width of 3 mm. The specimen's geometry and the loading procedure are illustrated in Figure 2a. Elongated U-notches with $a_0/d = 0,30$ (where a_0 represents the initial notch's length, while d is the depth of the specimen) were created under wet conditions one day prior to the test.

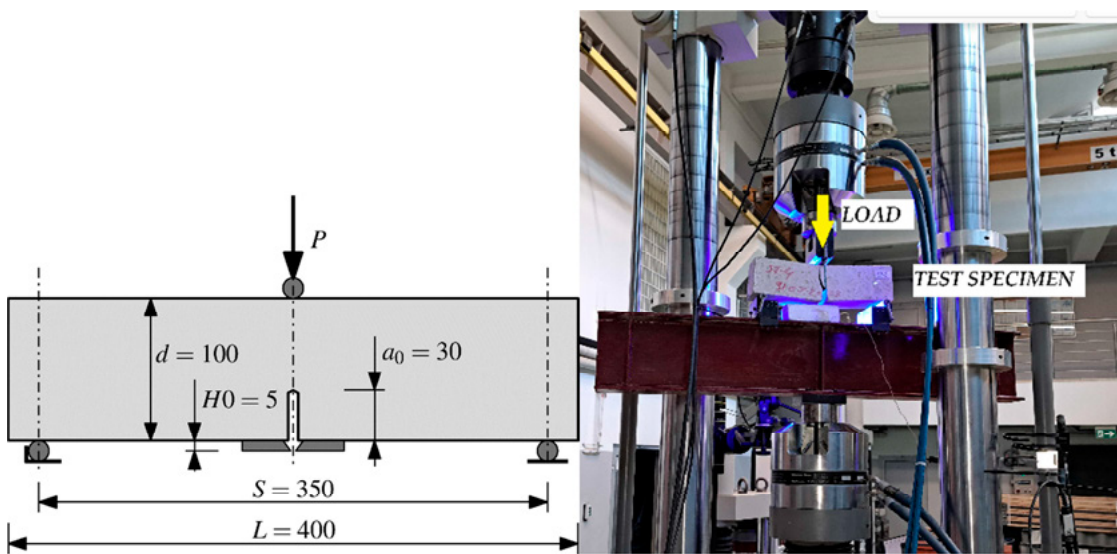


Figure 2. Test set-up for fracture testing: a) configuration and geometry, b) specimen during the test

The research was performed with the use of the hydraulic machine (Materials Test System, MTS; type 809; MTS Systems Corp.; Eden Prairie, MN, USA) and a gauge clip-on axial extensometer, placed on the clamping test grips. The details of the setup of the test apparatus are presented in Figure 2b. As a result of the experiment, the value of curve load (P) versus crack mouth opening displacement (CMOD) was recorded for all tested beam specimens.

The considered fracture parameters included critical stress intensity factor K_{Ic} and critical tip opening displacement $CTOD_c$. K_{Ic} is defined as the value of the stress intensity factor calculated at the critical effective crack tip using the measured maximum load, whereas $CTOD_c$ is the crack tip opening displacement. It is calculated at the original notch tip of the specimen using the measured maximum load and the critical effective crack length, i.e. a_c . A crack, initially of a given length (in this analysis $a_0 = 30$ mm), critically propagates when it reaches the length of a_c . The assessment of critical effective crack length a_c was conducted based on K_{Ic} and $CTOD_c$ values, employing the procedure and equations outlined in the RILEM TC 89-FMT (Shah, 1990). This procedure is based on the fracture model (TPFM) developed by Jenq and Shah (1985) and assumes a cyclic loading-unloading test approach. The practical use has been demonstrated by researchers, e.g. Bordelon (2007), Kosior-Kazberuk et al. (2018).

The digital image correlation (DIC) technique was applied to obtain the shape and trajectory of the crack paths in different concrete samples. This advanced measurement method allows the tracking of the cracking processes on the surface of concrete elements during the progressive crack propagation process in an accurate and precise manner. As a result, it is possible to distinguish subtle

differences in the shape of macro-cracks in relation to changes in the composition of the tested concretes. Performing such experiments makes it possible to obtain broad-scale information on the fracture characteristics of concrete. In addition, they constitute a valuable supplement to the results of tests of mechanical parameters of concrete.

Results of the research

Mechanical properties of concretes

The mechanical properties determined for concretes containing varying amounts of basalt minibars are presented in Table 3.

Table 3. Mechanical properties of concrete with basalt minibars – test results

Series	Type of cement	w/c	Compressive strength f_c		Flexural tensile strength $f_{ct,fl}$		Young's modulus E_{cm}	
			[MPa]		[MPa]		[GPa]	
M1	CEM I 42.5	0.5	58.12	1.8	6.06	1.8	38.82	0.25
M2			54.49	4.9	6.37	4.9	39.03	0.85
M3			48.37	11.2	6.59	11.2	41.14	0.84
M4			52.9	8.4	7.49	8.4	42.88	0.82
M5		0.4	55.76	5.2	6.09	5.2	40.31	0.63
M6			56.29	11.7	6.48	11.7	41.45	0.62
M7			53.1	2.1	7.86	2.1	43.39	0.85
M8			59.58	2.7	7.89	2.7	32.86	0.37
M9	CEM II 42.5R/ A-V	0.5	47.6	3.2	6.11	3.2	38.82	0.22
M10			53.37	4.1	6.32	4.1	38.1	0.49
M11			62.31	2.9	6.45	2.9	38.2	0.42
M12			60.32	8.5	6.54	8.5	42.88	0.28
M13		0.4	65.67	11.1	5.85	11.1	40.31	0.68
M14			59.77	5.7	6.11	5.7	41.45	0.17
M15			65.57	9.0	6.7	9.0	43.39	0.51
M16			63.44	4.8	7.23	4.8	43.42	0.21

The compressive strength and Young's modulus of concrete with basalt minibars increased negligibly compared to concrete without minibars. When the fibre content was raised to 4 kg/m³, a slight reduction in compressive strength was observed. The inclusion of fibres did not notably improve Young's modulus. On the other hand, these fibres had a pronounced effect on flexural tensile strength, which represents the load-bearing capacity at the first crack.

Figure 3 shows a typical cross-sectional after failure with a view of microbars that have been broken.

The following fracture parameters: critical stress intensity factor K_{Ic} , the critical value of crack tip opening displacement $CTOD_c$, and critical effective crack length a_c were determined based on P -CMOD curves. Selected load P versus CMOD curves obtained for concretes with basalt minibars are presented in Figure 4.



Figure 3. View of the cracked cross-section after failure

Fracture behavior of basalt minibars reinforced concrete

An analysis of the P - $CMOD$ curves revealed that the initial section of the curve is nearly linear for all the considered concrete types, with a slight increase in the strain of the notch tip under tension as the load increases. Following this linear portion, a deviation from linearity is observed, and the load reaches its maximum value, signifying the onset of crack initiation at the notch tip. The introduction of basalt minibars results in an extended segment length before reaching the peak load. Consequently, compared to control concrete, concretes with minibars reach the initial cracking load at higher $CMOD$ values. The impact of basalt minibars contents on the values of maximum load is somewhat ambiguous. The addition of basalt microbars to various series of concretes in quantities ranging from 2 kg/m^3 to 8 kg/m^3 resulted in the following impacts on test results:

- for CEMI 42.5 cement and water-to-cement ratio $w/c=0.5$, force P_{max} increased by 11%,
- for CEMI 42.5 cement and $w/c=0.4$, force P_{max} increased by 16%,
- for CEM II 42.5R/A-V cement and $w/c=0.5$, force P_{max} increase reached 29%, but there was a slight decrease in the case of concretes with 8 kg/m^3 of basalt minibars,
- for CEM II 42.5R/A-V cement and $w/c=0.4$, P_{max} increased by 25% when 2 kg/m^3 of fibers were used. However, it is worth noting that although the P_{max} value decreased with an increasing quantity of basalt minibars, the P_{max} value remained at least 15% higher compared to the reference concrete.

The post-critical phase of the P - $CMOD$ curve involves unloading initiated at 95% of the maximum load. Initially, load decreases with minimal $CMOD$ changes. Later, $CMOD$ decreases linearly until reaching the minimum load, followed by the next loading cycle. Subsequent cycles show significant changes in maximum load and $CMOD$ growth, with the control concrete exhibiting reduced maximum load in subsequent cycles. Analysis of concretes with basalt minibars reveals a transition from brittle to ductile behaviour, with strain softening and increased $CMOD$ at maximum load. $CMOD$ values are higher than control, indicating greater ductility. Changes in maximum load during cycles are less significant than the initial cycle, demonstrating enhanced ductility in basalt minibar concretes.

The primary advantage of the incorporation of basalt minibars into concrete is the improved ductility in the post-cracking region, as evident in the load- $CMOD$ plots. Increasing the fibre dosage significantly enhances the values of fracture parameters K_{IC} and $CTOD_c$. The obtained results, i.e. K_{IC} and $CTOD_c$, are shown in Figure 6.

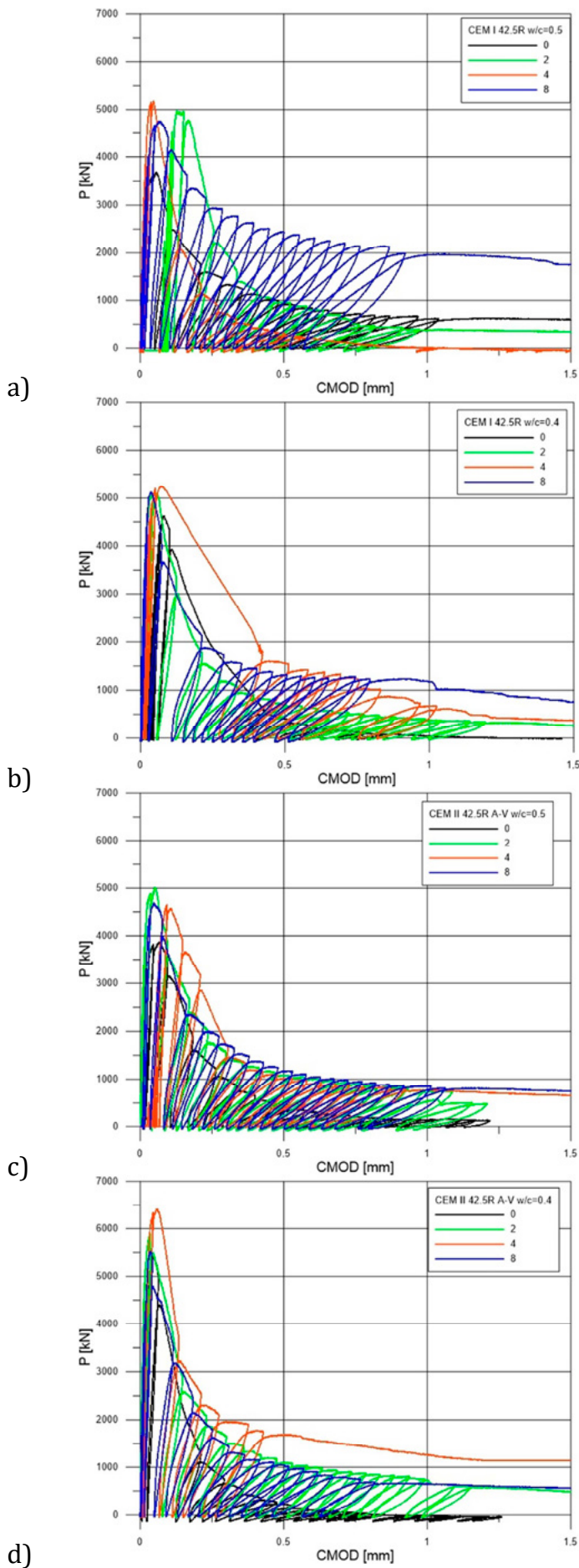


Figure 4. Load P versus CMOD curves for concretes with various content of basalt minibars: a) CEMI 42.5R $w/c = 0.5$, b) CEMI 42.5R $w/c = 0.4$, c) CEM II 42.5R/A-V $w/c = 0.5$, d) CEM II 42.5R/A-V $w/c = 0.5$

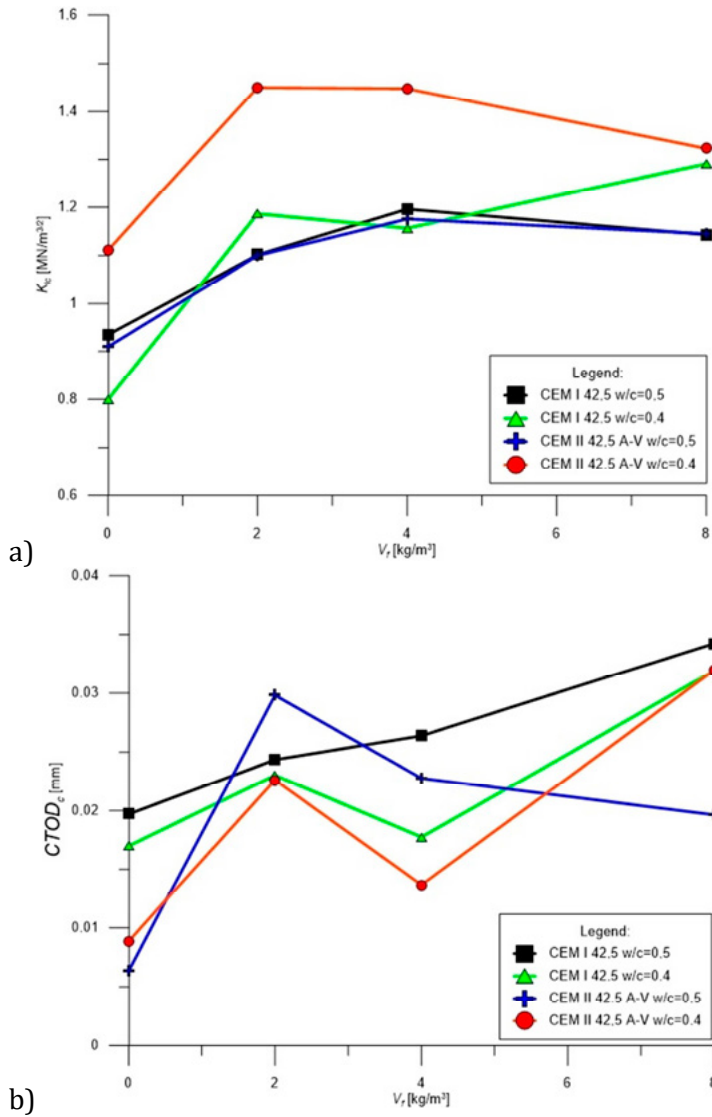


Figure 5. The influence of minibars content V_f [kg/m³], type of cement, and w/c ratio on a) the critical stress intensity factor K_{IC} [MN/mm^{3/2}], b) the critical value of crack tip opening displacement $CTOD_c$ [m]

Increasing the fibre content causes a significant increase in stress intensity factor K_{IC} , indicating greater cracking resistance of concrete. The most significant changes that occurred due to the introduction of fibres were observed in concretes made with CEM II/A-V 42.5R cement. The addition of minibars in contents of at least 2 kg/m³, compared to the control concrete without minibars, resulted in an increase in the K_{IC} value by at least 18, 48, 21, and 31%, depending on the type of cement and the w/c ratio. Increasing minibars content resulted in an increase in the K_{IC} factor was:

- for CEMI 42.5R concretes: for a w/c ratio of 0.5 , by 27%; for a w/c ratio of 0.4 , by 62%,
- for CEM II 42.5R/A-V concretes: for a w/c ratio of 0.5 , by 29%, for a w/c ratio of 0.4 by 30%.

Until the initiation of cracking, loads are transferred between the fibres and the cement matrix through adhesion forces, and both the fibres and the matrix remain in an elastic state. As the load increases continuously, some micro-cracks may develop until the deformations of the matrix reach the critical value, which is why $P-CMOD$ charts exhibit nonlinearity. Basalt minibars act like bridges in the cracks, transferring stresses, and thus, the test specimen remains in equilibrium. With further loading, minibars undergo cracking or are pulled out from the concrete matrix.

Toughness and macro-crack propagation

The next step of the analysis is a broader description of the manner of macro-crack propagation and the type of fracture for all the series of tested beams.

For the above purpose, diagnostics were performed both visually and with the use of the state-of-the-art and precise Digital Image Correlation (DIC) technique. Tables 4, 5, 6, and 7 present the specimens after the tests. The CMOD and CTOD values from the clip gauges were obtained directly from the measuring devices. However, as far as DIC analyses are concerned, virtual sensors for the measurement of crack opening width at the crack tip and at the beginning of the notch were introduced in the GOM Correlate software.

Table 4. Crack pattern was observed during the tests for concrete made with cement CEM I 42.5R $w/c = 0.5$

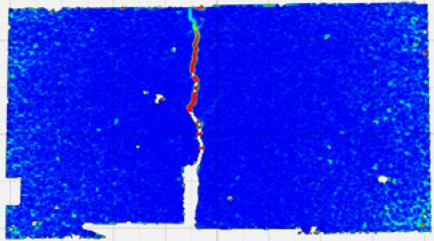
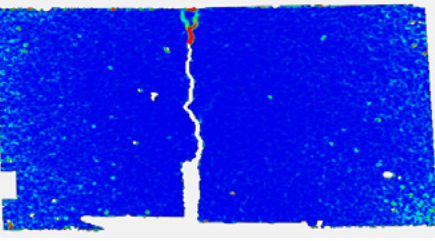
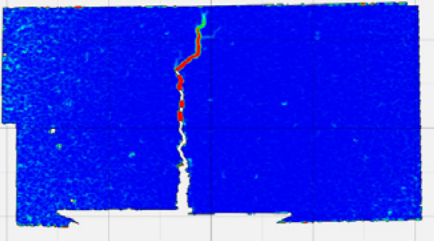
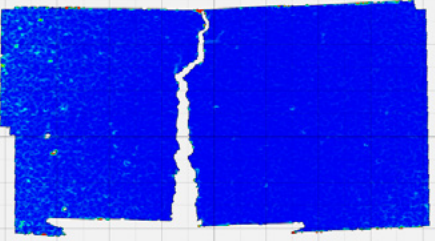
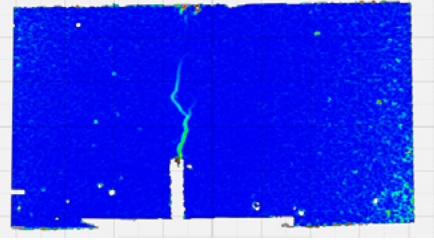
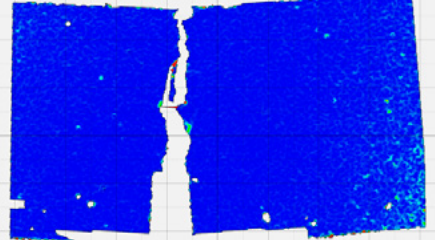
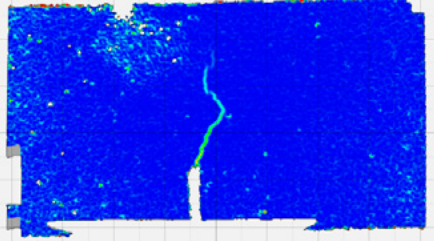
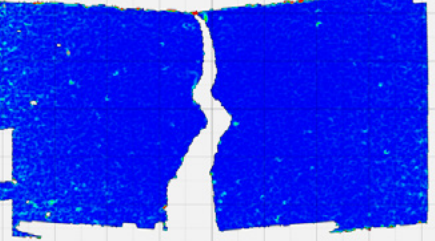
Series	Crack shapes observed in the tests using the digital image correlation (DIC) method when CMOD=0.5 mm	Crack shapes observed in the tests using the digital image correlation (DIC) method when CMOD=max
M1		
M2		
M3		
M4		

Table 5. The crack pattern observed in the tests of concrete made with cement CEM I 42.5R $w/c = 0.4$

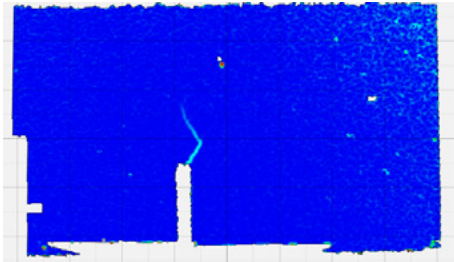
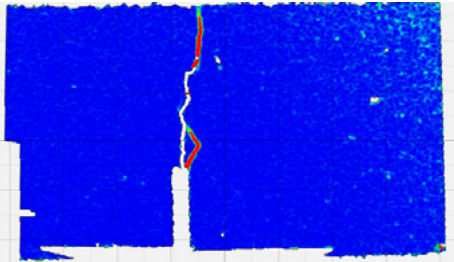
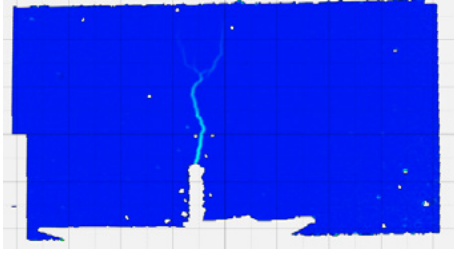
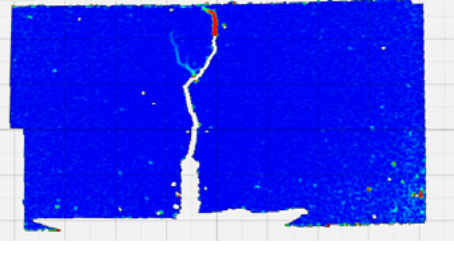
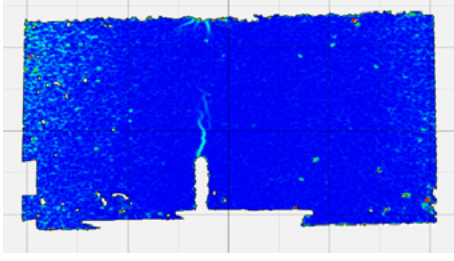
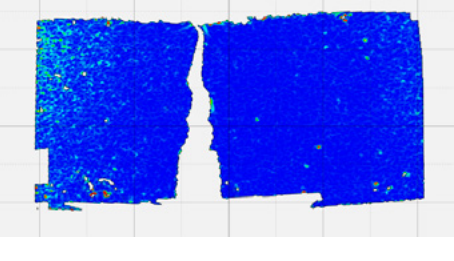
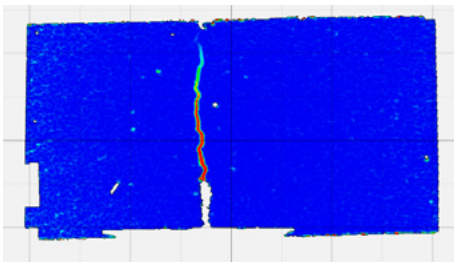
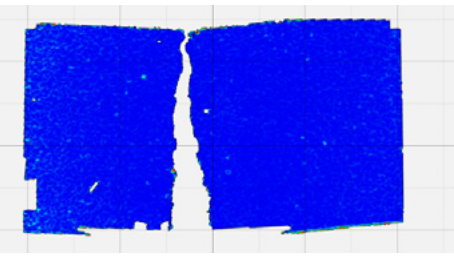
Series	Crack shapes observed in the tests using the digital image correlation (DIC) method when CMOD=0.5 mm	Crack shapes observed in the tests using the digital image correlation (DIC) method when CMOD=max
M5		
M6		
M7		
M8		

Table 6. The crack pattern observed in the tests of concrete made with cement CEM II A/V 42.5R $w/c = 0.5$

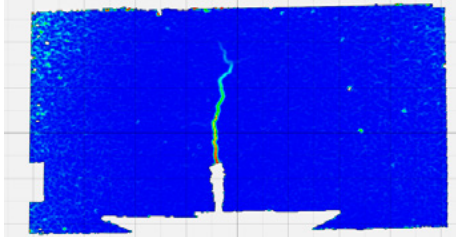
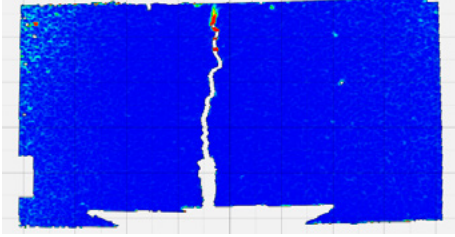
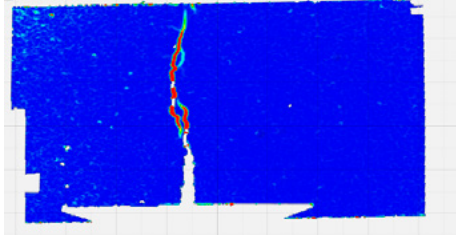
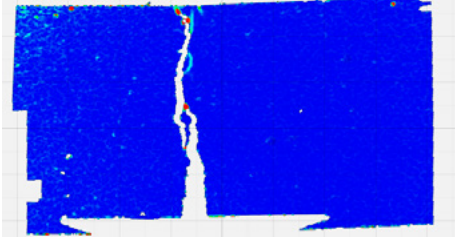
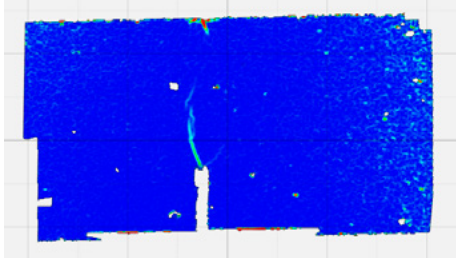
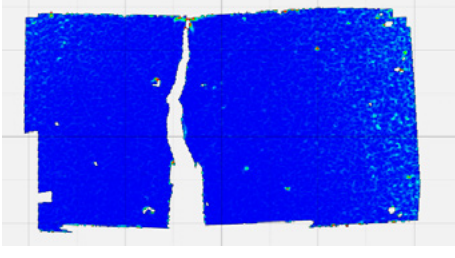
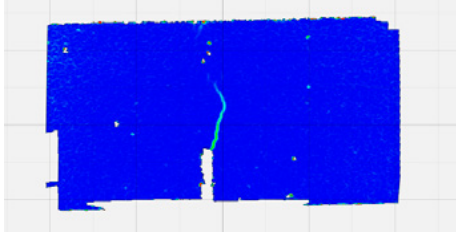
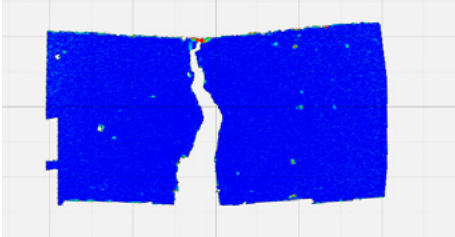
Series	Crack shapes observed in the tests using the digital image correlation (DIC) method when CMOD=0.5 mm	Crack shapes observed in the tests using the digital image correlation (DIC) method when CMOD=max
M9		
M10		
M11		
M12		

Table 7. The crack pattern observed in the tests of concrete made with cement CEM II A/V 42.5R $w/c = 0.4$

Series	Crack shapes observed in the tests using the digital image correlation (DIC) method when CMOD=0.5 mm	Crack shapes observed in the tests using the digital image correlation (DIC) method when CMOD=max
M13		
M14		
M15		
M16		

Beams typically failed due to a single large crack, more evident in plain concrete, while those with microbars showed quasi-plastic failure. Digital Image Correlation (DIC) confirmed this, with brittle concrete having straight cracks and more flexible ones exhibiting curved cracks with branches. The initial crack formation was sudden but detectable with DIC, followed by propagation and widening. Reinforced concretes showed ductility, carrying loads at increasing CMOD values, unlike plain concrete, which failed after reaching maximum load. All specimens cracked before CMOD reached 0,05 mm, and even at CMOD of around 0.5 mm, cracks extended to the upper surface, widening as CMOD increased.

Conclusions

The conclusion of the examined volume fractions of basalt minibars (i.e. 2, 4, and 8 kg/m³) exerted a significant impact on the fracture properties of concrete. At the same time, it only had a minimal effect on its strength properties apart from flexural strength. Basalt minibars can improve the frac-

ture parameters, such as K_{Ic} and $CTOD_c$, recorded at the point of maximum load. The analysis of the P-CMOD diagrams demonstrated a marked improvement in the post-peak fracture behaviour of concrete beams with the addition of basalt minibars. This improvement in both pre-peak and post-peak behaviour was evident in the changes observed in the plots P-CMOD. The results of the assessment of the toughness and characteristics of minibar-reinforced concrete indicated that concrete specimens incorporating basalt minibars exhibited significantly higher ductility and capacity compared to ordinary concrete specimens. The highest increases in values were observed in concrete using cement CEM II 42.5R/A-/V. The variations in fracture parameters and the alterations in fracture curves recorded under load underscore the ability of basalt minibars to resist crack propagation. This analysis of various parameters makes it possible to perform a comprehensive evaluation of the changes in the fracture resistance of quasi-brittle materials such as concrete. Strain maps make it possible to analyse the propagation and width of crack openings in the tested elements. This failure mode was more noticeable in plain concrete beams, while concrete beams modified by microbars exhibited a quasi-plastic failure mode. The tests carried out confirmed the possibility of strengthening concrete elements made of CEM II 42.5R A/V by introducing dispersed reinforcement in the form of basalt mini-bars.

Acknowledgements

The research leading to these results has received funding from the commissioned task entitled "VIA CARPATIA Universities of Technology Network named after the President of the Republic of Poland Lech Kaczyński", contract no. MEiN/2022/DPI/2577, action entitled "In the neighbourhood – inter-university research internships and study visits".

The contribution of the authors

Conceptualization, J.K., M.K.K., M.S. and A.A.; literature review, J.K. and A.A.; methodology, A.M.; formal analysis, J.K., M.K.K. and M.S.; writing, J.K., M.K.K., M.S. and A.A.; conclusions and discussion, J.K., M.K.K. and M.S.

The authors have read and agreed to the published version of the manuscript.

References

- Abbas Ashour Alaraza, H., Kharun, M., & Chiadighikaobi, P. C. (2022). The effect of minibars basalt fiber fraction on mechanical properties of high-performance concrete. *Cogent Engineering*, 9, 2136603. <https://doi.org/10.1080/23311916.2022.2136603>
- Batog, M., Bakalarz, J., Synowiec, K., & Dziuk, D. (2022). Stosowanie cementów wieloskładnikowych w budownictwie. *Budownictwo, Technologie, Architektura*, 3.
- Bordelon, A. C. (2007). *Fracture behavior of concrete materials for rigid pavements system* [Master Thesis]. University of Illinois at Urbana-Champaign. https://collections.lib.utah.edu/dl_files/84/76/8476870eec3fe0e68af4950a281444b11a5358d6.pdf
- Branston, J., Das, S., Kenno, S. Y., & Taylor, C. (2016a). Influence of basalt fibres on free and restrained plastic shrinkage. *Cement and Concrete Composites*, 74, 182-190. <https://doi.org/10.1016/j.cemconcomp.2016.10.004>
- Branston, J., Das, S., Kenno, S. Y., & Taylor, C. (2016b). Mechanical behaviour of basalt fibre reinforced concrete. *Construction and Building Materials*, 124, 878-886. <http://dx.doi.org/10.1016/j.conbuildmat.2016.08.009>
- Determination of the fracture energy of mortars and concretes by means of three-point bend tests on notched beams.* (1985). *Materials and Structures*, 18, 287-290. <https://doi.org/10.1007/BF02472918>
- EN 12350-2:2019. Testing fresh concrete. Slump test. <https://standards.iteh.ai/catalog/standards/cen/cf0e0511-2176-454c-948d-9e515f3a03f1/en-12350-2-2019>
- EN 12350-7:2019. TC – Tracked Changes. Testing fresh concrete. Air content. Pressure methods. <https://standards.iteh.ai/catalog/standards/cen/444b4a93-2e0f-41e7-96e9-7d25505d78bd/en-12350-7-2019>
- EN 12390-13:2013. Testing hardened concrete. Determination of secant modulus of elasticity in compression. <https://standards.iteh.ai/catalog/standards/cen/752cfc47-b32b-4c17-be4f-30dfee3af3ca/en-12390-13-2013>
- EN 12390-3:2009. Testing hardened concrete – Part 3: Compressive strength of test specimens. <https://standards.iteh.ai/catalog/standards/cen/d1d94876-958b-4941-ade0-780076fc330a/en-12390-3-2009>

- EN 12390-5:2019. Testing hardened concrete – Part 5: Flexural strength of test specimens. <https://standards.iteh.ai/catalog/standards/cen/5653c2c7-55a9-4bcb-8e13-5b1dfb0e3baf/en-12390-5-2019>
- Iyer, P., Kenno, S. Y., & Das, S. (2015). Mechanical Properties of Fiber-Reinforced Concrete Made with Basalt Filament Fibers. *Journal of Materials in Civil Engineering*, 27(11), 04015015. [https://doi.org/10.1061/\(ASCE\)MT.1943-5533.0001272](https://doi.org/10.1061/(ASCE)MT.1943-5533.0001272)
- Jenq, Y., & Shah, S. P. (1985). Two Parameter Fracture Model for Concrete. *Journal of Engineering Mechanics*, 111, 1227-1241. [https://doi.org/10.1061/\(ASCE\)0733-9399\(1985\)111:10\(1227\)](https://doi.org/10.1061/(ASCE)0733-9399(1985)111:10(1227))
- Jiang, C., Fan, K., Wu, F., & Chen, D. (2014). Experimental study on the mechanical properties and microstructure of chopped basalt fibre reinforced concrete. *Materials & Design*, 58, 187-193. <https://doi.org/10.1016/j.matdes.2014.01.056>
- Kabay, N. (2014). Abrasion resistance and fracture energy of concretes with basalt fiber. *Construction and Building Materials*, 50, 95-101. <https://doi.org/10.1016/j.conbuildmat.2013.09.040>
- Kosior-Kazberuk, M., Krassowska, J., Vidales Barriguete, A., & Ramirez, C. P. (2018). Fracture parameters of basalt fiber reinforced concrete. *Anales de Edificación*, 4(3), 52-58. <https://doi.org/10.20868/ade.2018.3800>
- Patnaik, A., Miller, L., Adhikari, S., & Standal, P. C. (2013). Basalt FRP Minibar Reinforced Concrete. *Proceedings of the Fibre Concrete 2013*, Prague, Czech Republic, 1-10. https://concrete.fsv.cvut.cz/fcproceedings/download/2013/Full_PATNAIK_Anil.pdf
- Shah, S. P. (1990). Size-effect method for determining fracture energy and process zone size of concrete. *Materials and Structures*, 23, 461-465. <https://doi.org/10.1007/BF02472030>
- Słowik, M. (2019). The analysis of failure in concrete and reinforced concrete beams with different reinforcement ratio. *Archive of Applied Mechanics*, 89, 885-895. <https://doi.org/10.1007/s00419-018-1476-5>
- Słowik, M., & Błazik-Borowa, E. (2011). Numerical study of fracture process zone width in concrete members. *Architecture Civil Engineering Environment*, 4(2), 73-78.
- Wei, B., Cao, H., & Song, S. (2010). Tensile behavior contrast of basalt and glass fibers after chemical treatment. *Materials & Design*, 31(9), 4244-4250. <https://doi.org/10.1016/j.matdes.2010.04.009>

Julita KRASSOWSKA • Marta KOSIOR-KAZBERUK • Marta SŁOWIK • Amanda AKRAM

ZROWNOWAŻONE PRZYSZŁOŚĆ BUDOWNICTWA I POTENCJAŁ BETONU ZE ZBROJENIEM W FORMIE MINIPRĘTÓW BAZALTOWYCH

STRESZCZENIE: W artykule przedstawiono wyniki badań wpływu mikroprętów bazaltowych na podkrytyczne i pokrytyczne zachowanie się elementów próbnych z betonu wykonanego z cementu niskoemisyjnego. Cementy niskoemisyjne to rodzaj cementów, które są produkowane z mniejszą emisją gazów cieplarnianych i innych zanieczyszczeń w porównaniu z tradycyjnymi cementami. Przeprowadzono analizy zmian parametrów mechaniki pęknięcia w zależności od zawartości mikroprętów w mieszance betonowej (0, 2, 4, 8 kg/m³), rodzaju zastosowanego cementu i wpływu wskaźnika w/c. Wykazano, że beton zbrojony mikroprętami bazaltowymi charakteryzuje się zwiększoną odpornością na inicjację i propagację pęknięć. Zaobserwowano wzrost współczynnika intensywności naprężeń dla betonów z cementu CEM I 42.5R o w/c = 0.5 o 27% w/c = 0.4 o 62%, oraz dla betonów z cementu CEM II 42.5R/A-V o w/c = 0.5 o 29% w/c = 0.4 aż o 30%. Wykazano, że dodatek mikroprętów do betonu wykonanego z cementu niskoemisyjnego znacząco zwiększa parametry mechaniczne tego materiału.

SŁOWA KLUCZOWE: beton, minipręty bazaltowe, mechanika pęknięcia betonu, zrównoważone budownictwo